



1 Interannual Variability of BVOC Emissions in an Alpine City

2 **Lisa Kaser¹, Arianna Peron¹, Martin Graus¹, Marcus Striednig¹, Georg Wohlfahrt², Stanislav**
3 **Juráň³, Thomas Karl¹**

4 ¹Department of Atmospheric and Cryospheric Sciences, University of Innsbruck, Innrain 52f, 6020
5 Innsbruck, Austria

6 ²Department of Ecology, University of Innsbruck, Sternwartestrasse. 15, 6020 Innsbruck, Austria

7 ³Global Change Research Institute of the Czech Academy of Sciences, Bělidla 986/4a, 603 00 Brno,
8 Czech Republic

9

10 *Correspondence to:* Thomas Karl (thomas.karl@uibk.ac.at) and Lisa Kaser (kaser.lisa@gmail.com)

11 **Abstract.** Terpenoid emissions above urban areas are a complex mix of biogenic and anthropogenic
12 emission sources. In line with previous studies we found that summertime terpenoid emissions in an
13 alpine city were dominated by biogenic sources, but especially at lower temperatures the anthropogenic
14 influences were non-negligible. Inter-seasonal emission measurements revealed consistency for
15 monoterpenes and sesquiterpenes, but a large difference in isoprene between the summers 2015 and
16 2018. Standardized emission potentials for monoterpenes and sesquiterpenes were $0.12 \text{ nmol m}^{-2} \text{ s}^{-1}$ and
17 $3.0 \cdot 10^{-3} \text{ nmol m}^{-2} \text{ s}^{-1}$ in 2015 and $0.11 \text{ nmol m}^{-2} \text{ s}^{-1}$ and $3.4 \cdot 10^{-3} \text{ nmol m}^{-2} \text{ s}^{-1}$ in 2018, respectively.
18 Observed isoprene emissions were about four times higher in 2018 than in 2015. This factor decreased
19 to 2.3 after standardizing isoprene emissions to 30°C air temperature and photosynthetic active radiation
20 (PAR) of $1000 \mu\text{mol m}^{-2} \text{ s}^{-1}$. Based on emission model parameterizations, increased leaf temperatures
21 can explained ~50% of these differences, but standard emission potentials remained higher in 2018,
22 when a heat wave persisted. Potential other reasons for the differences such as emission
23 parameterization, footprint changes, water stress conditions and tree trimming are investigated.

24 1 Introduction

25 Biogenic and anthropogenic volatile organic compounds (BVOCs, AVOCs) in the atmosphere can
26 contribute to surface air pollution both due to their influence on tropospheric ozone formation and due
27 to their potential to act as precursors for secondary organic aerosol formation (Derwent et al., 1996,
28 Fehsenfeld et al., 1992, Fuentes et al., 2000, Goldstein et al., 2009, Laothawornkitkul et al., 2009,
29 Riipinen et al., 2012). BVOCs are playing a particularly important role globally, as their emission
30 strength is estimated to be 10 times larger than AVOCs (Guenther et al., 2012, Piccot et al., 1992). Also,
31 many BVOCs are characterized as highly reactive (Atkinson and Arey, 2003, Fuentes et al., 2000),
32 resulting in rapid peroxy radical chemistry important for ozone and ultra-fine particle formation



33 processes (Simon et al., 2020). Of the total global BVOC emissions, terpenes dominate, with 50%
34 attributed to isoprene, 15% to monoterpenes and about 0.5% to sesquiterpenes (Guenther et al., 2012).
35 In forests with predominating isoprene emissions, isoprene was found responsible for 50-100% of the
36 tropospheric ozone production (Duene et al., 2002, Tsigaridis and Kanakidou, 2002, Poisson et al.,
37 2001). In coniferous forests monoterpene and sesquiterpene emissions often dominate (Johansson and
38 Janson, 1993, Thunis and Cuvelier, 2000, Juráň et al., 2017). It has been shown that RO₂ self-reactions
39 of monoterpenes and sesquiterpenes can rapidly create highly oxidized matter (HOM) and are a key
40 player for new particle formation (NPF) events in forests under low NO_x conditions (Simon et al.,
41 2020).

42 In urban environments where the mixture of BVOCs and AVOCs is more complex, several recent
43 studies point out the importance of biogenic emissions for local air quality (Simon et al., 2019, Bonn et
44 al., 2018, Churkina et al., 2017, Ren et al., 2017, Papiez et al., 2009, Chameides et al., 1988) and that
45 the BVOC influence is especially high during summertime heat waves (Churkina et al. 2017).
46 Particularly in summer, biogenic sources are dominating in urban environments. E.g., Yadav et al.
47 (2019) found an increased importance of biogenic isoprene in an urban site in western India during pre-
48 monsoon season when temperatures and PAR were high, Hellen et al. (2012) found a strong biogenic
49 influence on isoprene and monoterpene concentrations in Helsinki in July. Summertime isoprene in two
50 large Greek cities was appointed with PMF to come 60-70% from vegetation (Kaltsonoudis et al. 2016).
51 Yang et al. (2005) showed a strong seasonal and daily cycle in isoprene contributing it therefore to
52 biogenic sources in an urban region in Taiwan. Borbon et al (2002) showed that biogenic sources
53 strongly superimpose the traffic emissions of isoprene in summer in an urban area in France. Wagner
54 and Kuttler (2014) found that during summer afternoons in an urban area in Germany anthropogenic
55 influences on isoprene concentrations were negligible. Chang et al. (2014) and Wang et al. (2013)
56 showed that in a tropical-subtropical metropolis biogenic contributions overwhelmed anthropogenic
57 contributions of isoprene in summer and that biogenic sources started to dominate in all seasons above a
58 threshold temperature of 17-21°C. Whereas all so far cited studies were based on concentration
59 measurements where the influence can be both local and regional and strongly modulated by
60 atmospheric dilution the following studies were based on eddy covariance flux tower sites: At
61 temperatures over 25°C more than 50% of the isoprene flux was found to be biogenic in origin in
62 London with a mean daytime flux of 0.18 mg m⁻² h⁻¹ (Langford et al. 2010). Similarly, Valach et al.
63 (2015) in a different study in London found a mean daytime flux of 0.2 mg m⁻² h⁻¹. Kota et al. (2014)
64 found a daytime median flux of 2.1 mg m⁻² h⁻¹ over Houston, Texas and contributed it to mostly
65 biogenic sources. Park et al (2010) found also in Houston, Texas a daytime isoprene flux of 0.7 mg m⁻²
66 h⁻¹. Rantala et al. (2016) found that 80% of the measured 10 ng m⁻² s⁻¹ summer daytime isoprene flux
67 near Helsinki could be contributed to biogenic sources by comparing emissions at low and high
68 temperatures.

69 While there is evidence for urban trees to have positive influence on urban environments such as
70 mitigating the urban heat island effect, sequestering CO₂ and particles as well as acting as storm water
71 interception (Escobedo et al., 2011, Connop et al., 2016, Livesley et al., 2016), BVOC emissions of
72 urban trees and their subsequent effect on air pollution is very plant species dependent (Corchnoy et al.,
73 1992, Steinbrecher et al., 2009, Fitzky et al., 2019) and should be taken into account when planting
74 urban trees (Calfapietra et al., 2013, Churkina et al., 2015, Ren et al., 2017). Emerging evidence that



75 isoprene derived RO₂ competes with RO₂ radicals from higher molecular weight terpenes in the
76 formation of new particles highlights the need to study emissions in different environments (Berndt et
77 al. 2018).
78 To assess the status quo of BVOC emissions in a city or area and their impact on local air quality urban
79 eddy covariance flux measurements have become available for some urban areas (Langford et al. 2010,
80 Park et al 2010, Kota et al. 2014, Valach et al. 2015, Rantala et al. 2016).
81 Few studies characterize the seasonal and interannual changes of BVOCs and even fewer studies are
82 available in urban environments: Chang et al. (2014) measured seasonal changes in urban isoprene
83 concentrations in Taipei revealing the biogenic dominance of isoprene in daytime concentrations of
84 biogenic sources for spring, summer and fall and even a dominance of biogenic sources at night in
85 summer. Valach et al. (2015) showed decreasing isoprene fluxes transitioning from summer to winter at
86 a central London measurement site. Vaughan et al. (2017) report airborne flux measurements over
87 South Sussex of two consecutive summers showing different isoprene emissions that can be explained
88 by different temperature and cloud cover conditions. Warneke et al. (2010) tried to explain the
89 measured interannual differences of a factor of 2 in emissions of isoprene and monoterpene over Texas
90 by temperature, drought effects or influences from changes in leaf area index (LAI). Palmer et al.
91 (2006) found a maximum of 20-30% interannual difference in isoprene emissions using satellite-based
92 isoprene quantification from formaldehyde measurements over North America. A model study by
93 Steinbrecher et al. (2009) found only a 10% annual difference in biogenic emissions from cold to hot
94 years. Gulden et al. (2007) found that, on a regional scale, variations in leaf biomass density driven by
95 variations in precipitation are together with temperature and shortwave radiation variations the most
96 important factors for variations in BVOC emissions. Tawfik et al. (2012) found in a model study that
97 interannual variation of isoprene emission is with 18% strongest in July with temperature and soil
98 moisture explaining 80% of the variations, whereas the influences of variations in photosynthetic active
99 radiation (PAR) and LAI were negligible. In a three-year study over a northern hardwood forest,
100 Pressley et al. (2005) found that total cumulative isoprene emissions varied only by 10%.
101 Given the current lack of multi-year urban VOC flux measurements and our limited understanding of
102 the interannual variability of biogenic and anthropogenic emission sources, the objective of the present
103 study was to quantify the interannual variation of the urban ecosystem-atmosphere exchange of the
104 three major isoprenoids, isoprene, monoterpenes and sesquiterpenes, and to analyze the underlying
105 drivers. We hypothesized (i) that the exchange of these BVOCs can be attributed largely to the spatio-
106 temporal variability of biogenic sources and (ii) that differences in environmental forcings are the main
107 drivers of interannual variability. To address these hypotheses, urban eddy covariance BVOC flux
108 measurements during two growing seasons above the city of Innsbruck (Austria) are blended with
109 bottom-up emission estimates based on a process-based model and a detailed urban tree inventory.



110 **2 Materials and methods**

111 **2.1 Field site and instruments**

112 VOC concentrations and flux measurements were conducted during two comparable summer periods
113 (July 10–September 9 2015 & July 27–September 2 2018) close to the city center of Innsbruck on the
114 rooftop of one of the tallest buildings in the area. Details on the Innsbruck Atmospheric Observatory
115 (IAO) measurement site and instrument performance were published by Karl et al. (2018) and Striednig
116 et al. (2020). Therefore, we give here only a short summary of the study location and measurement

117 details. The measurement location ($47^{\circ} 15' 51.66''$ N, $11^{\circ} 23' 06.82''$ E) is shown in Figure 1A on a
118 1000x1000m map surrounding the site. This will in the following be referred to as the study area. The
119 dominant wind direction at the IAO is NE during the daytime and SW during nighttime (Karl et al.
120 2020, Striednig et al. 2020).

121 3D sonic wind, CO₂, and H₂O were measured with a CPEC200 (Campbell Scientific) eddy covariance
122 system on a tower on top of the building 42 m above street level. A heated inlet line led from the tower
123 to a close-by laboratory hosting a PTR-QiTOF-MS instrument (IONICON Analytik, Sulzer et al. 2014).
124 Both summers the PTR-QiTOF-MS was operated in H₃O⁺ mode with standard drift tube conditions of
125 112 Townsend (E/N electric field strength). Regular instrument calibrations and zeroing revealed
126 typical acetone and isoprene sensitivities of 1550 and 950 Hz/ppbv respectively. 3D wind and VOCs
127 were sampled at 10 Hz.

128 Incident PAR was calculated from short wave radiation measured by a pyranometer (Schenk 8101,
129 Schenk, Wien) applying the relationship derived by Jacovides et al. (2003).

130 Precipitation data were collected 400 m south of our field site by a MPS TRWS 503 tipping bucket
131 precipitation gauge and a Thies 5.4103.10.000 precipitation monitor, mounted at 1.5 m above a grass
132 surface.

133 Plant available soil moisture for 2015–2019 was retrieved as the SMAP level 4 3-hourly 9 km rootzone
134 soil moisture product (Reichle et al. 2018) via the AppEEARS interface
135 (<https://lpdaacsvc.cr.usgs.gov/appears/>).

136 **2.2 Eddy covariance fluxes**

137 This study focuses on biogenic emissions collected during summer 2015 and summer 2018. As biogenic
138 emissions are strongly light- and temperature-driven, the total available dataset was reduced to daytime
139 hours (9:00–16:00 local time) and mean wind directions from 0°–120°. Data with wind direction from
140 the south and exceeding a wind speed > 10 m/s were excluded as they can be attributed to foehn events.

141 Eddy covariance fluxes were calculated using a MATLAB[®] code described by Striednig et al. (2020).
142 As a QA/QC criteria for fluxes we implemented a combination of steady state filter of the respective
143 scalar, the integral turbulence characteristics test of the wind components and flow sector filtering,
144 similar to the combination described in Chapter 4.2.5. in Foken (2017) with a required overall quality
145 class of 6 or lower. According to Foken (2017), classes 1–6 can be used for long-term measurements of
146 fluxes without limitations.

147 Footprint and footprint density were calculated following Kljun et al. (2015).



148 We standardized isoprene eddy covariance fluxes $E_{0,ISO}$, to a temperature of 303.15 K and PAR of 1000
149 $\mu\text{mol m}^{-2} \text{s}^{-1}$ using a model described in detail by Guenther et al. (2006): $E_{ISO} = E_{0,ISO} * \gamma_T * \gamma_P$, where
150 γ_T and γ_P are temperature- and light-dependent coefficients respectively containing current and past
151 (24h and 240h) conditions. In order to investigate relative inter-seasonal changes of isoprene emissions
152 the MEGAN 5-layer canopy model (Guenther et al., 2006) was applied.

153 Monoterpene and sesquiterpene eddy covariance fluxes are known to be purely temperature dependent
154 and can be described as: $E_{MT} = E_{0,MT} * C_{T,MT}$ and $E_{SQT} = E_{0,SQT} * C_{T,SQT}$ where C_T is a temperature
155 dependent factor described by Guenther et al. (1994).

156 In the case of sesquiterpenes, turbulent time scales (100 s) are on the order of chemical time scales as
157 sesquiterpenes can react fast with ozone (typical ozone concentrations were 30 ppbv). The chemical loss
158 was estimated by the following equation: $c(t)/c_0 = \exp(-t_{\text{turb}}/t_{\text{chem}})$ where t_{turb} is the turbulent time scale
159 and t_{chem} the chemical time scale.

160 **2.3 City tree inventory**

161 An inventory of all trees planted by the city municipality is available for the city of Innsbruck, Austria
162 containing location, tree species, diameter at breast height and height. However, this inventory does not
163 include trees from private gardens. Therefore, all accessible trees from private gardens were identified
164 and added to the existing tree inventory. The location of the trees from the city inventory and private
165 gardens in the study area are shown in Figure 1A. Within the study area a total of 1904 registered trees
166 distributed across 129 tree species were counted. A list of the 44 most abundant tree species, where the
167 species count in the study area was 6 or more, is given in Table 1.

168 **2.4 Emission potentials**

169 Literature values of plant-species specific emission potentials of isoprene and monoterpene, in μg
170 compound g^{-1} dry-weight h^{-1} standardized to 303.15 K and PAR 1000 $\mu\text{mol m}^{-2} \text{s}^{-1}$ were assigned to the
171 44 most abundant species in the study area. This includes all tree species with an occurrence larger than
172 6 individuals within the footprint and accounts for ~90% of the total counted trees. Emission potential
173 assignment was based on the detailed work by Stewart et al. (2003) for the overlapping species. Other
174 emission potentials were taken from other literature and if more than one literature value was available,
175 an average was taken. All species, emission potentials and references thereof are shown in Table 1.
176 Sesquiterpene (SQT) emission potentials were taken from Karl et al. (2009) and if not reported therein
177 the average value of 0.1 μg compound g^{-1} dry-weight h^{-1} was assigned.

178 **2.5 Relative IS, MT, SQT emission ratio maps**

179 To generate emission ratio maps, the study area was divided into a 100 m by 100 m grid and tree
180 species were counted in each grid tile and multiplied by their emission potential listed in Table 1. The
181 resulting map in units of μg compound g^{-1} dry-weight h^{-1} neglects the actual, but unknown, amount of
182 dry leaf weight of each individual tree.

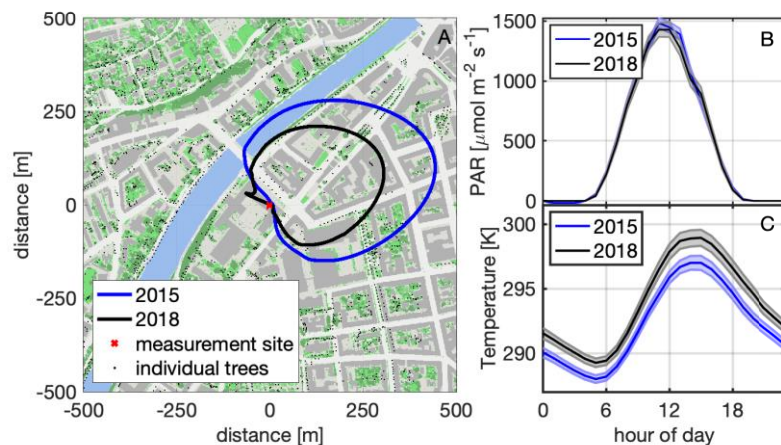


183 Due to the unknown amount of emitting leaf material, it is difficult to compare bottom-up estimates
184 from this method with direct eddy covariance flux measurements. A more robust comparison is possible
185 when relative emission maps are investigated such as ISO/MT, ISO/SQT and SQT/MT. For this we first
186 added up all individual tree emission factors in each tile (e.g. $ISO_{square} = \sum ISO_{tree}$) and then divided
187 these by the tile emission factors e.g. ISO_{tile}/MT_{tile} . For simplicity this is in the following called
188 ISO/MT. ISO/MT is then multiplied with the footprint density in each tile and summed up over the total
189 study area. This is a bottom-up ISO/MT ratio expected at the measurement site.

190 3 Results and discussion

191 3.1 Flux footprint, light & temperature conditions

192 The flux footprint of the daytime data at the IAO is shown in Figure 1A plotted on a map of 1000 m x
193 1000 m surrounding the flux tower location. 60% of the flux footprint density lay, in both years, entirely
194 within the study area. The footprint area extended slightly farther in 2015 than in 2018. The relative
195 contribution of the land cover types in both years however was similar with 40-41% buildings, 23%
196 paved areas, 25-28% roads, 5% trees, 5% short vegetation, and <1% water. Within the 60% flux
197 footprint area in 2015 and 2018 lay 148 and 89 individual trees of the tree inventory distributed over 33
198 and 24 tree species, respectively. Combining the tree inventory with literature values on basal emission
199 factors (Table 1) and the footprint density calculated for each tree location revealed that 60% and 70%
200 of the bottom-up isoprene emissions arriving at the flux tower were from 12 trees in 2015 and 2018
201 respectively. These were trees closest to the footprint density maximum and trees with high isoprene
202 basal emission factors. The tree species were *Populus nigra*, *Platanus acerifolia*, *Sophora japonica*, and
203 *Quercus robur*. As the footprint area was smaller in 2018 compared to 2015, the relative importance of
204 the emission of these trees was higher in 2018 than in 2015. Bottom-up monoterpene emissions were
205 distributed more evenly among different tree species: 19 trees in the study area accounted for ~50% of
206 the bottom-up MT emissions arriving at the flux tower. The most important species were *Aesculus*
207 *carnea*, *Pinus sylvestris*, *Larix decidua*, and *Acer platanoides*. Sesquiterpene bottom-up emissions were
208 even more equally distributed over the tree species: 38 trees accounted for 50% and 60% of bottom-up
209 SQT emissions arriving at the flux tower in 2015 and 2018 respectively. *Betula pendula* and *Sophora*
210 *japonica* contributed 20% and 12% to the emissions arriving at the tower in 2015 and 22% and 19% in
211 2018. Diurnal cycles of PAR and air temperature, two of the strongest biogenic emission drivers, are
212 shown in Figure 1B and 1C, respectively. While PAR was very similar during the two summers, mean
213 air temperatures in 2018 were 2K higher during daytime and 1.5K higher during nighttime compared to
214 2015. The higher temperatures in 2018 coincided with an intense heat wave. Monthly average
215 temperatures in August 2018 were 3K above the climatological mean values (1981-2010).
216



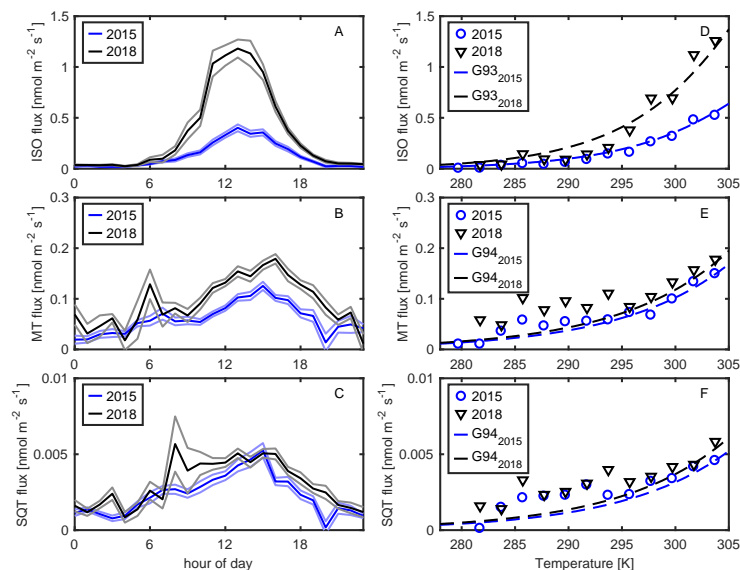
217
218 **Figure 1:** A) Map surrounding the Innsbruck Atmospheric Observatory (indicated with a red cross in the center) depicting trees,
219 short vegetation, water, roads, paved areas and buildings in dark green, light green, blue, white, light grey and dark grey
220 respectively. Black dots represent individual trees from the city tree inventory. The 60% daytime (9:00-16:00) footprint areas with
221 mean wind directions between 0° and 120° are shown in blue and black for summer 2015 and 2018 respectively. B) Diurnal cycle of
222 average and standard error of PAR. C) Diurnal cycle of average and standard error of ambient temperature 2015 (blue) and
223 2018 (black) Maps were created in Matlab (www.mathworks.com) and are based on OpenStreetMap
224 (<https://www.openstreetmap.org/copyright>) under the CC BY 3.0 AT license.

225 3.2 Two summers of urban BVOC fluxes

226 Biogenic isoprene emissions are light and temperature dependent (e.g. Guenther et al. 1993), while
227 biogenic monoterpene and sesquiterpene emissions are mostly temperature dependent (e.g. Guenther et
228 al. 1994). Karl et al. (2018) showed that isoprene and monoterpene at this measurement site are linked
229 to biogenic processes. Figure 2 A-C shows the average diurnal cycles of isoprene, monoterpene and
230 sesquiterpene fluxes. Daytime maxima of isoprene emissions were $0.4 \text{ nmol m}^{-2} \text{ s}^{-1}$ and $1.2 \text{ nmol m}^{-2} \text{ s}^{-1}$
231 in 2015 and 2018 respectively. Estimates based on winter-time benzene/isoprene flux ratios reveal that
232 an upper limit of 20-30% of the daytime isoprene flux was anthropogenic in origin and the larger
233 isoprene source at this site was biogenic. This is in good accordance with previous studies conducted in
234 urban environments (Kota et al. 2014, Park et al 2010, Rantala et al. 2016). The large interannual
235 difference and its potential reasons are discussed further in section 3.3.

236 Maximum average daytime monoterpene fluxes were $0.13 \text{ nmol m}^{-2} \text{ s}^{-1}$ and $0.18 \text{ nmol m}^{-2} \text{ s}^{-1}$ for 2015
237 and 2018, respectively, and average daytime sesquiterpene fluxes were $5 \cdot 10^{-3} \text{ nmol m}^{-2} \text{ s}^{-1}$ in both years.
238 All data binned into 2K temperature ranges of all three species and both summers are shown in Figure 2
239 D-F. Fig. 2D shows a good match with the theoretical temperature curve from Guenther et al. (1993) for
240 isoprene emissions of both summers. The interannual difference, discussed further in section 3.3,
241 persisted at higher temperatures. Measured monoterpene and sesquiterpene measured fluxes at lower
242 temperatures (280K-295K) were higher than the predicted values based on the Guenther et al. (1994)
243 algorithm. This could be an indication that at lower temperatures other, non-biogenic sources
244 contributed to monoterpene and sesquiterpene fluxes at this site. At temperatures higher than 295K, MT
245 and SQT fluxes followed known temperature dependencies.
246

247 Standardizing the fluxes removes the variability due to current temperature and light conditions and
248 allows for interannual comparison as well as comparison to other studies. Standardized isoprene fluxes
249 (standardized to 303.15K and PAR 1000 $\mu\text{mol m}^{-2}\text{s}^{-1}$ not including 24h and 240h temperature and
250 light history) were $0.58\pm 0.01\text{ nmol m}^{-2}\text{s}^{-1}$ and $1.33\pm 0.06\text{ nmol m}^{-2}\text{s}^{-1}$ in 2015 and 2018 respectively.
251 Isoprene fluxes from both years were lower than what Rantala et al. (2016) found for an urban flux site
252 in Helsinki, where the standardized emission potential was $125\text{ ng m}^{-2}\text{s}^{-1}$ (eq. to: $1.8\text{ nmol m}^{-2}\text{s}^{-1}$). The
253 Helsinki flux site had a larger vegetation cover of 38-59% compared to our study area, where the
254 vegetation cover was estimated to be 10% within the flux footprint. Park et al. (2010) reported a
255 standard emission rate of isoprene of $0.53\text{ mg m}^{-2}\text{h}^{-1}$ (eq. to: $2.2\text{ nmol m}^{-2}\text{s}^{-1}$) over Houston, Texas,
256 which is higher than both our 2018 and 2015 measurements. This is potentially due to a higher
257 vegetation cover in Houston as well as strong isoprene-emitting oaks within the footprint of the
258 measurement site. Valach et al. (2015) reported a daytime average flux in August of $0.3\text{ mg m}^{-2}\text{h}^{-1}$ (eq.
259 to: $1.2\text{ nmol m}^{-2}\text{s}^{-1}$) at an urban site in London and Acton et al. (2020) a summer daytime average
260 isoprene flux of $4.6\text{ nmol m}^{-2}\text{s}^{-1}$ at an urban site in Beijing, both however cannot be directly compared
261 to our measurements as their values were not standardized to temperature and PAR.
262 Average daytime standardized monoterpene fluxes were, with 0.12 and $0.11\text{ nmol m}^{-2}\text{s}^{-1}$ in 2015 and
263 2018, respectively, relatively similar between the two summers. Average daytime standardized
264 sesquiterpene fluxes were over a magnitude smaller than standardized monoterpene fluxes and were
265 comparable between the two summers with mid-day values on the order of $3.0\cdot 10^{-3}\text{ nmol m}^{-2}\text{s}^{-1}$ and
266 $3.5\cdot 10^{-3}\text{ nmol m}^{-2}\text{s}^{-1}$ in 2015 and 2018 respectively. As the turbulent time scale and the chemical
267 lifetime of sesquiterpenes with respect to destruction by ozone were similar, we calculated an upper
268 limit of the correction factor of 2.5. This means that, when correcting for reactive losses of
269 sesquiterpenes with ozone, sesquiterpene emissions could have been up to 2.5 times higher than the
270 measured values leading to an upper limit of daytime standardized sesquiterpene emission of $7.5\cdot 10^{-3}$
271 $\text{nmol m}^{-2}\text{s}^{-1}$ and $8.8\cdot 10^{-3}\text{ nmol m}^{-2}\text{s}^{-1}$ in 2015 and 2018, respectively.
272



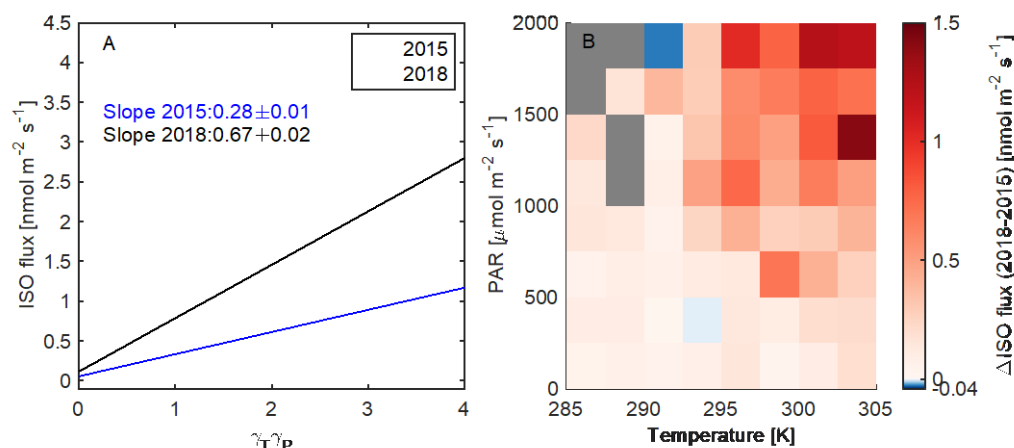
274
275
276
277
278

Figure 2: Diurnal cycles of average isoprene (A), monoterpene (B) and sesquiterpene (C) fluxes for the summers 2015 (blue) & 2018 (black), shaded areas indicate the standard error. (D-F) show temperature binned isoprene, monoterpene and sesquiterpene fluxes respectively. The dashed lines depict the theoretical temperature behavior based on Guenther et al. (1993) (G93) and Guenther et al. (1994) (G94) normalized to the respective fluxes at 303.15K.

279 3.3 Isoprene flux anomaly

280 The isoprene flux difference measured between the two summers of 2015 and 2018 is shown in Figure 2
281 A and D. Figure 2D represents the isoprene dependence on temperature. (Guenther et al. 1993). Monson
282 and Fall (1989) found isoprene fluxes not only to depend on current temperature conditions, but also on
283 current light conditions. In addition, past 24h and 240h temperature and light conditions play a role (e.g.
284 Guenther et al., 2006). These theoretical temperature and light parameters are plotted vs. the observed
285 isoprene flux in Figure 3A based on the MEGAN big leaf approach (Guenther et al., 2006). Even after
286 including both actual and past temperature and light parameters the difference in isoprene emissions
287 between the two summers could not be resolved and standardized emission factors were still a factor 2.4
288 higher in 2018 than in 2015. Figure 3B shows that the difference was increasing with higher
289 temperature and higher PAR values.

290



291
292
293
294
295
296

Figure 3: A) Theoretical temperature and light dependencies (Guenther et al. 2006) including T_{24} , T_{240} , P_{24} , P_{240} vs. observed isoprene flux in 2015 (blue) and 2018 (black). The lines indicate a linear fit with fit parameters displayed within the plot. The slope of the fit parameter represents the standardized (303.15 K and 1000 PAR) isoprene emission factors. B) Isoprene flux differences between 2018 and 2015 binned by temperature and PAR, positive differences are shown in red, negative in blue and bins with no available data are colored grey.

297
298
299
300
301
302

In contrast to monoterpene and sesquiterpene emissions, which exhibited comparable emission potentials between the two years and are mainly driven by evaporative emissions from storage reservoirs (e.g. Kesselmeier and Staudt, 1999), it remains a puzzle why the isoprene emission potential was substantially higher in 2018 compared to 2015. As neither actual temperature and light dependencies nor 24h and 240h past temperature and light could explain the observed differences in



isoprene fluxes, we investigated the following potential reasons: a) variation in the flux footprint, b) tree trimming, c) water availability/drought, and d) emission parameterization.

- a) As shown in Figure 1A the footprint area in 2018 was smaller than the footprint in 2015. Possible reasons for this are a change in flux tower position between the two years by ~50 m, as well as different meteorological conditions. Median wind directions were 71° and 68° and wind speeds 1.6 m/s and 1.8 m/s in 2015 and 2018 respectively. The median Obukhov length was -26 m and -49 m in 2015 and 2018 respectively. Multiplying the footprint density at each tree location with the basal emission factor of each tree species revealed a potential difference of 24% higher isoprene emissions in 2018 than in 2015. Even though the actual leaf area of each individual tree is not known and therefore neglected, this 24% of potential emission difference due to footprint changes cannot explain the factor of 2.4 in observed emissions between the two years. This analysis assumes that the trees from the tree inventory were responsible for the majority of isoprene emissions and that they were more important than emissions from short vegetation (e.g. lawn). Further supporting evidence that the flux footprint change cannot fully explain the observed differences derives from the fact that both monoterpenes and sesquiterpenes did not show significant inter-annual variations in their normalized emission potentials.
- b) A second possible explanation for the isoprene flux difference could be that trees underwent different trimming in the growing seasons which could lead to a different LAI in the two seasons. Personal communications from city gardeners revealed that of the trees most important for isoprene emissions in the study area (*Populus nigra*, *Populus alba*, *Quercus robur*) only poplar trees were cut differently in 2015 than in 2018. In 2015 only dead wood was removed from the poplars, whereas trees were cut more substantially in 2018. This would however lead to an expected smaller flux in 2018 than in 2015 due to reductions in leaf area.
- c) A third possible explanation is that the growing season of 2018 was exceptionally dry with lower-than-average precipitation and satellite-derived rootzone soil moisture (Figure 4A and 4B). Concurrent water flux observations, however, shown in Fig. 4C, indicate that on average the 2018 daytime summer water flux was 0.2 mmol m⁻² s⁻¹ higher than in 2015. Also the total surface water vapor conductance was 50 mmol m⁻² s⁻¹ higher in 2018 than in 2015. Higher water fluxes observed in 2018 agree with anecdotal reports of city trees being artificially watered throughout the summer. Water fluxes in urban areas (maximum Bowen ratios observed in Innsbruck: 6 (Karl et al., 2020)) are generally very low (e.g. 5-6 times lower) when compared to measurements over purely vegetated surfaces, and therefore notoriously difficult to interpret. As such we cannot exclude the possibility of processes other than evapotranspiration from city trees contributing to higher water fluxes observed in 2018. An obvious explanation is that a significant water runoff during extensive watering operations resulted in increased evaporation over hot asphalt and other non-vegetated surfaces, leading to higher water fluxes in 2018. Water was also applied to asphalt surfaces more frequently during mornings to minimize the effect of urban aerosol pollution.

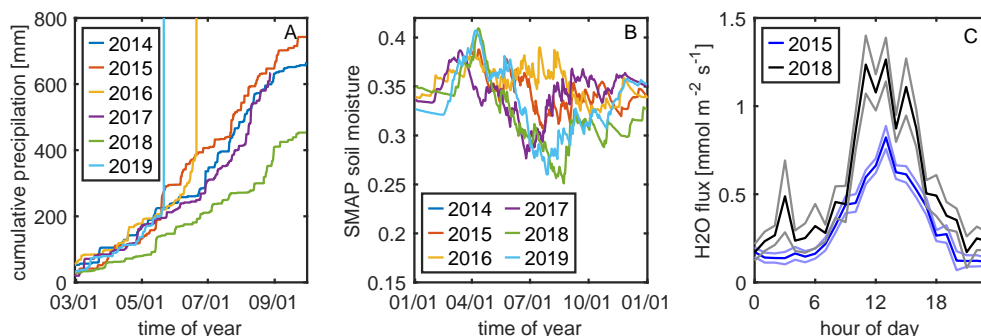
It is well established that isoprene production in plants can decouple from photosynthesis during periods of drought and can be sustained by alternative metabolic carbon sources (e.g. Bertin & Staudt, 1996; Pegoraro et al., 2004a,b; Fortunati et al., 2008; Genard-Zielinski et al., 2014;



Potosnak et al., 2014; Wu et al., 2015). The exact reason for biochemical regulation of isoprene emissions during drought is not fully unraveled, but has been suggested to represent a response for coping with heat stress (Loreto et al., 1998). Isoprene fluxes were observed to increase during the very early onset of drought conditions. For example, Seco et al. (2015) reported an increase in the ecosystem scale isoprene emission potential about one month before significant changes in pre-dawn leaf water potential were observed, but when CO₂ uptake was already decreasing. Additionally, they observed that the closing of stomata had a bigger effect on CO₂ than water fluxes, because gradual increases of vapor pressure deficit during the evening offset reduced leaf conductance. Isoprene is not controlled by stomata and would not be influenced by any changes in stomatal opening. In addition, their canopy scale observations suggested a shift of the temperature maximum of isoprene emissions towards higher temperatures from pre-drought to drought conditions. Ferracci et al. (2020) reported a threefold increase in the isoprene emission potential during the same 2018 heat wave in a UK oak forest. They also observed a stronger temperature dependence of isoprene emissions during the heat wave. We speculate that the 50-60% increase of the isoprene emission potential observed here, could have similar reasons, but this remains to be confirmed by detailed leaf gas exchange experiments.

- d) We also examined the impact of emission parameterization on isoprene emissions. Due to the lack of soil water content data, which would be hard to interpret in an urban context, the drought effect was not included in the emission model parameterization. Precipitation (Fig. 4A) and soil moisture data (Fig. 4B) suggest 2018 being drier than 2015, corresponding to a significant heat wave in the summer of 2018. Mild to severe drought conditions would reduce isoprene emissions further and therefore could not explain an increased isoprene emission potential in 2018. The fact that evaporative water fluxes however were comparable between 2015 and 2018 (and if at all were somewhat higher in 2018), suggest that the trees might not have undergone a severe drought episode in both years. To investigate relative changes in modelled emission parameterizations we set up the MEGAN 5-layer canopy model (Guenther et al., 2006) for different scenarios. We observed that a shift in T_{opt} towards higher temperatures helped minimize the observed difference between the two years (e.g. 10% to 40%). As an example, the diurnal daily isoprene flux differed between 2015 and 2018 by a factor of 3.8, and the 5 layer model with T_{opt} set to 313 K could explain about half of the flux enhancement. This would leave isoprene emission fluxes underestimated by about 50% in 2018.

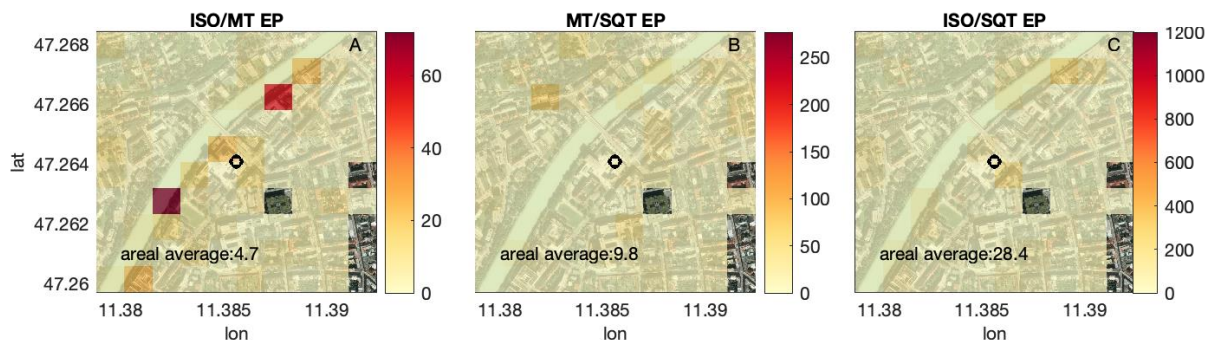
In contrast to isoprene, temperature dependence algorithms accurately predict increases of monoterpenes and sesquiterpenes due to increased temperatures in 2018 compared to 2015 (Fig. 2. B, C). This can be rationalized by the fact that monoterpenes and sesquiterpenes are primarily released from storage pools (Kesselmeier and Staudt, 1999), and temperature dependent changes in vapor pressures of these compounds are accurately predicted between 2015 and 2018.



381
382 **Figure 4:** A) cumulative precipitation for the growing seasons of 2014-2019 B) annual SMAP satellite soil moisture of the rootzone
383 from 2014-2019. C) diurnal cycle of water fluxes measured in 2015 (blue) and 2018 (black).

384 3.4 Top-down and bottom-up BVOC flux ratios

385 Standardized flux ratios were calculated to allow for a better comparison with bottom-up estimates
386 based on literature values of branch level emissions and a city tree inventory. Top-down (eddy
387 covariance) ISO_S/MT_S ratios were on the order of 5 in 2015 and 12 in 2018, again revealing a strong
388 difference between the two years. Top-down MT_S/SQT_S flux ratios were in the order of 30-40 before
389 factoring in losses of sesquiterpenes due to reactions with ozone. Factoring in the upper bound of
390 chemical loss correction, MT_S/SQT_S flux ratios could have been as low as 12-16. Top-down ISO_S/SQT_S
391 flux ratios lay on the order of 190 in 2015 and 380 in 2018, which was mostly caused by the difference
392 in ISO_S flux between the two years. The lower bounds of the ISO_S/SQT_S flux ratios due to fast reaction
393 of sesquiterpene with ozone were 80 and 150 for 2015 and 2018, respectively.
394 Branch-level standardized emissions are collected from the literature in Table 1 and are used to
395 calculate a bottom-up emission map shown in Figures 5 A-C. The 2018 footprint area (Fig. 1A) and
396 therefore footprint density was different to 2015. Combining bottom-up emission estimates with
397 footprint density functions, the theoretically expected ISO/MT, MT/SQT and ISO/SQT ratios in 2015
398 were 3.6, 5.1 and 18.7 respectively. Applying the 2018 footprint density, the values were slightly
399 different with 4.2, 4.6 and 19.2 for ISO/MT, MT/SQT and ISO/SQT ratios respectively.
400 The bottom-up ISO/MT emission ratio was close to the top-down ratio of 2015. This indicates again
401 that 2018 was an exceptional year. In contrast, the bottom-up MT/SQT and ISO/SQT emission ratios
402 were significantly lower than both summers top-down measured flux ratios. Even after accounting for
403 the chemical loss of sesquiterpene before it reached the point of measurement at the top of the building,
404 the bottom-up estimates were still higher than the top-down measured flux ratios. Literature values for
405 leaf level sesquiterpene emissions are rare and were for many species estimated in Table 1. Further
406 extensive studies on sesquiterpene standardized emissions for a large variety of plant species is needed
407 to close the gap between bottom-up and top-down emission ratio estimates.



408

409

410

411

Figure 5: A-C Bottom-up estimates of standardized ISO/MT, MT/SQT and ISO/SQT emission ratios based on literature values (see Table 1). Maps were created in Matlab (www.mathworks.com) and are based on OpenStreetMap (<https://www.openstreetmap.org/copyright>) under the CC BY 3.0 AT license.

412

4 Summary

413

414

415

416

417

418

419

420

421

422

423

424

425

426

427

In this study we found a strong correlation of isoprene fluxes with temperature as well as isoprene fluxes following the previously observed leaf-level light dependency. A correlation between isoprene and benzene fluxes in early spring before the start of the vegetation period can be extrapolated to the summer months. This resulted in a maximum of 20-30% influence of anthropogenic sources on isoprene emissions during both 2015 and 2018 summer measurement periods. A PMF analysis at this site (Karl et al. 2018) revealed two biogenic factors: one light- and temperature-dependent for isoprene and a second mostly temperature-dependent including monoterpenes and sesquiterpenes. The here presented temperature dependency of monoterpene and sesquiterpene fluxes reveals a potential anthropogenic source at temperatures lower than 295K as the fluxes below this temperature lay above the predicted temperature curves based on leaf level measurements (Guenther et al. 1994). Bottom-up emission estimates based on a city tree inventory and emission factors from literature showed a reasonable agreement to standardized ISO/MT flux ratios and an underestimation of standardized MT/SQT and ISO/SQT flux ratios. As there are only few literature values for laboratory-based standardized sesquiterpene emissions, this discrepancy motivates further studies to be able to resolve this gap between bottom-up and top-down emission ratios.

428

429

430

431

432

433

434

435

436

437

Interannual comparison of biogenic fluxes revealed up to four times higher isoprene fluxes in 2018, when a heat wave persisted, than in 2015. Monoterpene emissions were an order of magnitude lower than isoprene emissions and sesquiterpene emissions were another order of magnitude lower than monoterpene emissions, however both summer emissions were comparable for these two terpenoid classes after standardization of temperature. Normalizing isoprene fluxes to standard light conditions did not fully remove the interannual difference but decreased the factor to 2.4. The difference increased with higher temperature and higher PAR values. Analysis of footprint, water availability and pruning activity differences of the two summers did not resolve the observed differences in isoprene fluxes. Detailed analysis using standard emission modeling concepts suggested a higher-than-expected variation of urban isoprene emission potentials during the heat wave in 2018. While water flux



438 measurements did not indicate a severe drought in 2018, the effect of an intense heatwave in 2018 (2K
439 higher temperatures on average compared to 2015), likely resulted in enhanced isoprene emissions.
440 Isoprene emissions during drought stress have been grouped into two distinct phases (Niinemets, 2010,
441 Potosnak et al., 2014), and can be enhanced under pre-drought conditions (Seco et al., 2015, Ferracci et
442 al., 2020). Enhanced leaf temperatures (e.g. Potosnak et al., 2014) can explain part of the variance in
443 isoprene emissions, but significant differences remained. In addition to the leaf temperature effect,
444 Tattini et al., (2015) reported an upregulation of isoprene emissions during drought stress as antioxidant
445 defense in *Platanus x acerifolia* plants. If generalized, our observations could suggest distinct
446 differences that urban trees experience, possibly due to significantly altered environmental conditions
447 (e.g. stresses, light and temperature environment), which standard big leaf models might not fully
448 capture. Vegetation in urban areas is exposed to a variety of different atmospheric conditions, for
449 example the urban heat island effect, high levels of NO_y, heavy metal deposition or high loadings of
450 aerosols (e.g. black soot). Isoprene emissions have been linked to the plant's nitrogen metabolism (e.g.
451 Rosenstiel et al., 2008), where higher leaf nitrate can lead to lower isoprene emissions. Nitrogen dioxide
452 concentrations have been falling in Innsbruck and were 20% lower in 2018 than in 2015. Effects of air
453 pollutants on leaf surface characteristics and senescence were also reported in the past (Jochner et al.
454 2015; Honour et al., 2009), but a quantitative understanding of the impacts on isoprene emissions
455 remains unclear. Our observations suggest that more work is needed to improve our understanding of
456 urban biogenic isoprene emissions.

457 **Acknowledgements**

458 This work was primarily funded by the Hochschulraum-Strukturmittel (HRSM) funds sponsored by the Austrian Federal
459 Ministry of education, science and research (<https://www.bmbwf.gv.at/>), the EC Seventh Framework Program (Marie Curie
460 Reintegration Program, "ALP-AIR," Grant 334084), and partly by the Austrian National Science Fund (FWF) grants P30600
461 and P 33701. L.K received funding through the University of Innsbruck. S.J. was supported by the project SustES -
462 Adaptation strategies for sustainable ecosystem services and food security under adverse environmental conditions
463 (CZ.02.1.01/0.0/0.0/16_019/0000797). We used atmospheric data from the Innsbruck/University TAWES station, provided
464 by the Austrian Weather Service ZAMG and the Department of Atmospheric and Cryospheric Sciences, Universitat
465 Innsbruck. The City of Innsbruck is acknowledged for making the city tree inventory available, Michael Steiner for
466 complementing it with trees in private spaces.
467

468 **Conflict of Interest**

469 There is no conflict of interest.

470 **Code and Data availability**

471 The eddy covariance flux code used to analyze fluxes can be accessed via Github
472 (<https://git.uibk.ac.at/acinn/apc/innflux>). Data can be shared upon request.



473 **Author contributions**

474 LK and TK designed and conceived the manuscript. MG was leading the instrumental operation of the PTR-
475 TOF-MS for the 2015 and 2018 campaigns. MG, SJ, AP and MS performed the raw data processing of NMVOC
476 data. MS, TK and MG performed the NMVOC flux analysis. GW provided input on tree species information. TK
477 and LK performed analysis regarding BVOC emission modeling. SJ aided in the operation of the PTRTOFMS
478 and raw data processing of NMVOC data for the 2018 campaign. All authors provided input and contributed to
479 writing the manuscript.
480

481 **References**

- 482 Acton, W. J. F., Huang, Z., Davison, B., Drysdale, W. S., Fu, P., Hollaway, M., Langford, B., Lee, J.,
483 Liu, Y., Metzger, S., Mullinger, N., Nemitz, E., Reeves, C. E., Squires, F. A., Vaughan, A. R., Wang,
484 X., Wang, Z., Wild, O., Zhang, Q., Zhang, Y., and Hewitt, C. N.: Surface–atmosphere fluxes of volatile
485 organic compounds in Beijing, *Atmos. Chem. Phys.*, 20, 15101–15125, [https://doi.org/10.5194/acp-20-](https://doi.org/10.5194/acp-20-15101-2020)
486 15101-2020, 2020.
487
488 Atkinson, R. and Arey, J.: Gas-phase tropospheric chemistry of bio- genic volatile organic compounds:
489 a review, *Atmos. Environ.*, 37, Supplement 2, 197–219, [https://doi.org/10.1016/S1352-2310\(03\)00391-](https://doi.org/10.1016/S1352-2310(03)00391-1)
490 1, 2003.
491
492 Baghi, R., D. Helmig, A. Guenther, T. Duhl, and R. Daly: Contribution of flowering trees to urban
493 atmospheric biogenic volatile organic compound emissions, *Biogeosciences*, 9, 3777-3785,
494 <https://doi.org/10.5194/bg-9-3777-2012>, 2012.
495
496 Berndt, T., Mentler, B., Scholz, W., Fischer, L., Herrmann, H., Kulmala, M. and Hansel, A.: Accretion
497 Product Formation from Ozonolysis and OH Radical Reaction of α -Pinene: Mechanistic Insight and the
498 Influence of Isoprene and Ethylene, *Environ. Sci. Technol.*, 52 (19), 11069-11077,
499 <https://doi.org/10.1021/acs.est.8b02210>, 2018.
500
501 Bertin, N. and Staudt, M.: Effect of water stress on monoterpene emissions from young potted holm oak
502 (*Quercus ilex* L.) trees, *Oecologia*, 107, 456–462, <https://www.jstor.org/stable/4221358>, 1996.
503
504 Bonn, B., von Schneidemesser, E., Butler, T., Churkina, G., Ehlers, C., Grote, R., Klemp, D., Nothard,
505 R., Schäfer, K., von Stülpnagel, A., Kerschbaumer, A., Yousefpour, R., Fountoukis, C. and Lawrence,
506 M. G.: Impact of vegetative emissions on urban ozone and biogenic secondary organic aerosol: Box
507 model study for Berlin, Germany, *J. Clean. Prod.*, 176, 827-841,
508 <https://doi.org/10.1016/j.jclepro.2017.12.164>, 2018.
509



- 510 Borbon, A., Locoge, N., Veillerot, M., Galloo, J. C. and Guillermo, R.: Characterisation of NMHCs in a
511 French urban atmosphere: overview of the main sources, *Sci. Total Environ.*, 292, 3, 177-191,
512 [https://doi.org/10.1016/S0048-9697\(01\)01106-8](https://doi.org/10.1016/S0048-9697(01)01106-8), 2002.
513
- 514 Chameides, W.L., Lindsay, R.W., Richardson, J. and Kiang, C.S.: The role of biogenic hydrocarbons in
515 urban photochemical smog: Atlanta as a case study, *Science*, 241, 1473-1475,
516 <https://doi.org/10.1126/science.3420404>, 1988.
517
- 518 Chang, C.-C., Wang, J.-L., Lung, S.-C. C., Chang, C.-Y., Lee, P.-J., Chew, C., Liao, W.-C., Chen, W.-
519 N. and Ou-Yang, C.-F.: Seasonal characteristics of biogenic and anthropogenic isoprene in tropical–
520 subtropical urban environments, *Atmos. Environ.*, 99, 298-308,
521 <https://doi.org/10.1016/j.atmosenv.2014.09.019>, 2014.
522
- 523 Churkina, G., Kuik, F., Bonn, B., Lauer, A., Grote, R., Tomiak, K. and Butler, T.: Effect of VOC
524 emissions from vegetation on air quality in Berlin during a heatwave, *Environ. Sci. Technol.*, 51, S.
525 6120– 6130, <https://doi.org/10.1021/acs.est.6b06514>, 2017.
526
- 527 Churkina, G., Grote, R., Butler, T.M. and Lawrence, M.: Natural selection? Picking the right trees for
528 urban greening, *Environ. Sci. Policy*, 47, 12-17, <https://doi.org/10.1016/j.envsci.2014.10.014>, 2015
529
- 530 Calfapietra, C., Pallozzi, E., Lusini, I., and Velikova, V: Modification of BVOC emissions by changes
531 in atmospheric CO₂ and air pollution, *Biology, Controls and Models of Tree Volatile Organic*
532 *Compound Emissions*. (Dortrecht: Springer), 253–284, 2013.
533
- 534 Connop, S., Vandergert, P., Eisenberg, B., Collier, M. J., Nash, C., Clough, J., and Newport, D.:
535 Renaturing cities using a regionally-focused biodiversity-led multifunctional benefits approach to urban
536 green infrastructure, *Environ. Sci. Policy*, 62, 99–111, <https://doi.org/10.1016/j.envsci.2016.01.013>,
537 2016.
538
- 539 Corchnoy, S.B., Arey, J. and Atkinson, R.: Hydrocarbon emission from twelve urban shade trees of the
540 Los Angeles, California, Air Basin, *Atmos. Environ.*, 26 B, 339e348, [https://doi.org/10.1016/0957-1272\(92\)90009-H](https://doi.org/10.1016/0957-1272(92)90009-H), 1992.
541
- 542
- 543 Derwent, R. G., Jenkin, M. E. and Saunders, S. M.: Photochemical ozone creation potentials for a large
544 number of reactive hydrocarbons under European conditions, *Atmos. Environ.*, 30:181–99,
545 [doi:10.1016/1352-2310\(95\)00303-G](https://doi.org/10.1016/1352-2310(95)00303-G), 1996.
546
- 547 Duane, M., Poma, B., Rembges, D., Astorga, C. and Larsen, B.R.: Isoprene and its degradation products
548 as strong ozone precursors in Insubria, Northern Italy, *Atmos. Environ.*, 36, 3867-3879,
549 [https://doi.org/10.1016/S1352-2310\(02\)00359-X](https://doi.org/10.1016/S1352-2310(02)00359-X), 2002.
550



- 551 Escobedo, F. J., Kroeger, T., and Wagner, J. E.: Urban forests and pollution mitigation: analyzing
552 ecosystem services and disservices, *Environ. Pollut.*, 159, 2078–2087,
553 <https://doi.org/10.1016/j.envpol.2011.01.010>, 2011.
554
- 555 Fehsenfeld, F., Calvert, J., Goldan, P., Guenther, A.B., Hewitt, C.N., Lamb, B., Liu, S., Trainer, M.,
556 Westberg, H., and Zimmerman, P.: Emissions of volatile organic compounds from vegetation and the
557 implications for atmospheric chemistry, *Global Biogeochem. Cy.* 6, 389e430,
558 <https://doi.org/10.1029/92GB02125>, 1992.
559
- 560 Fuentes, J.D., Lerdau, M., Atkinson, R., Baldocchi, D., Botteneheim, J.W., Ciccioli, P., Lamb, B.,
561 Geron, C., Gu, L., Guenther, A., Sharkey, T.D., and Stockwell, W.: Biogenic hydrocarbons in the
562 atmosphere boundary layer: a review, *B. Am. Meteorol. Soc.* 81, 1537e1575,
563 [https://doi.org/10.1175/1520-0477\(2000\)081<1537:BHITAB>2.3.CO;2](https://doi.org/10.1175/1520-0477(2000)081<1537:BHITAB>2.3.CO;2), 2000.
564
- 565 Ferracci, V., Bolas, C. G., Freshwater, R. A., Staniaszek, Z., King, T., Jaars, K., Otu-Larbi, F., Beale, J.,
566 Malhi, Y., Waine, T. W., Jones, R. L., Ashworth. K. and Harris, N. R. P.: Continuous isoprene
567 measurements in a UK temperate forest for a whole growing season: Effects of drought stress during the
568 2018 heatwave, *Geophys. Res. Lett.*, 47, e2020GL088885. <https://doi.org/10.1029/2020GL088885>,
569 2020.
570
- 571 Fitzky, A. C., Sandén, H., Karl, T., Fares, S., Calfapietra, C., Grote, R., Saunier, A. and Rewald B.: The
572 Interplay Between Ozone and Urban Vegetation—BVOC Emissions, Ozone
573 Deposition, and Tree Ecophysiology, *Front. For. Glob. Change*, 2:50.
574 <https://doi.org/10.3389/ffgc.2019.00050>, 2019.
575
- 576 Foken, T.: *Micrometrology*, Springer Berlin Heidelberg, <https://doi.org/10.1007/978-3-540-74666-9>,
577 2007.
578
- 579 Fortunati, A., Barta, C., Brilli, F., Centritto, M., Zimmer, I., Schnitzler, J.-P. and Loreto, F.: Isoprene
580 emission is not temperature-dependent during and after severe drought-stress: a physiological and
581 biochemical analysis, *The Plant Journal*, 55, 687-697, [https://doi.org/10.1111/j.1365-](https://doi.org/10.1111/j.1365-313X.2008.03538.x)
582 [313X.2008.03538.x](https://doi.org/10.1111/j.1365-313X.2008.03538.x), 2008.
583
- 584 Fuentes, J., Lerdau, M., Atkinson, R., Baldocchi, D., Bottenheim, J., Ciccioli, P., Lamb, B., Geron, C.,
585 Gu, L., Guenther, A., Sharkey, T., and W, S.: Biogenic hydrocarbons in the atmospheric bound- ary
586 layer: a review, *B. Am. Meteorol. Soc.*, 81, 1537–1575, doi:10.1175/1520-
587 [0477\(2000\)081<1537:BHITAB>2.3.CO;2](https://doi.org/10.1175/1520-0477(2000)081<1537:BHITAB>2.3.CO;2), 2000.
588
- 589 Genard-Zielinski, A.-C., Ormeño, E., Boissard, C. and Fernandez, C.: Isoprene emissions from Downy
590 oak under water limitation during an entire growing season: What cost for growth?, *PLoS ONE*, 9,
591 e112418, <https://doi.org/10.1371/journal.pone.0112418>, 2014.
592



- 593 Goldstein, A.H., Koven, C.D., Heald, C.L. and Fung, I.Y.: Biogenic carbon and anthropogenic
594 pollutants combine to form a cooling haze over the southeastern United States, PNAS, 106, 1-6,
595 <https://doi.org/10.1073/pnas.0904128106>, 2009.
- 596
597 Guenther, A., Zimmerman, P., Harley, P., Monson, R. and Fall, R.: Isoprene and monoterpene emission
598 rate variability: Model evaluations and sensitivity analysis, J. Geophys. Res., 98, 12609-12617,
599 <https://doi.org/10.1029/93JD00527>, 1993.
- 600
601 Guenther, A., Zimmerman, P., and Wildermuth, M.: Natural VolatileOrganic-Compound Emission Rate
602 Estimates for United-States Woodland Landscapes, Atmos. Environ., 28, 1197–1210,
603 [https://doi.org/10.1016/1352-2310\(94\)90297-6](https://doi.org/10.1016/1352-2310(94)90297-6), 1994.
- 604
605 Guenther, A., Karl, T., Harley, P., Wiedinmyer, C., Palmer, P. I., and Geron, C.: Estimates of global
606 terrestrial isoprene emissions using MEGAN (Model of Emissions of Gases and Aerosols from Nature),
607 Atmos. Chem. Phys., 6, 3181–3210, <https://doi.org/10.5194/acp-6-3181-2006>, 2006.
- 608
609 Guenther, A. B., Jiang, X., Heald, C. L., Sakulyanontvittaya, T., Duhl, T., Emmons, L. K., and Wang,
610 X.: The Model of Emissions of Gases and Aerosols from Nature version 2.1 (MEGAN2.1): an extended
611 and updated framework for modeling biogenic emissions, Geosci. Model Dev., 5, 1471–1492,
612 <https://doi.org/10.5194/gmd-5-1471-2012>, 2012.
- 613
614 Gulden, L. E., Yang, Z. L. and Niu, G. Y.: Interannual variation in biogenic emissions on a regional
615 scale, J. Geophys. Res.-Atmos., 112, D14103, <https://doi.org/10.1029/2006JD008231>, 2007.
- 616
617 Hellen, H., Tykkä, T. and Hakola, H.: Importance of monoterpenes and isoprene in urban air in northern
618 Europe, Atmos. Environ., 59, 59-66, <https://doi.org/10.1016/j.atmosenv.2012.04.049>, 2012.
- 619
620 Honour, S. L., Bell, J. N. B., Ashenden, T. W., Cape, J. N., and Power, S. A: Responses of herbaceous
621 plants to urban air pollution: Effects on growth, phenology and leaf surface characteristics, Environ.
622 Pollution, 157, 1279-1286, <https://doi.org/10.1016/j.envpol.2008.11.049>, 2009.
- 623
624 Jacovides, C., Tymvios, F., Asimakopoulos, D., Theofilou, K. M. and Pashiardes, S.: Global
625 photosynthetically active radiation and its relationship with global solar radiation in the Eastern
626 Mediterranean basin, Theor. Appl. Climatol., 74, 227–233, <https://doi.org/10.1007/s00704-002-0685-5>,
627 2003.
- 628
629 Jochner, S., Markevych, I., Beck, I., Traidl-Hoffmann, C., Heinrich, J., and Menzel, A.: The effects of
630 short- and long-term air pollutants on plant phenology and leaf characteristics, Environ. Pollution, 206,
631 382-389, <https://doi.org/10.1016/j.envpol.2015.07.040>, 2015.
- 632



- 633 Johansson, C. and Janson, R.W.: Diurnal cycle of O₃ and monoterpenes in a coniferous forest:
634 Importance of atmospheric stability, surface exchange, and chemistry, *J. Geophys. Res.*, 9, 5121-5134,
635 <https://doi.org/10.1029/92JD02829>, 1993.
636
- 637 Juráň, S., Pallozzi, E., Guidolotti, G., Fares, S., Šigut, L., Calfapietra, C., Alivernini, A., Savi, F.,
638 Večeřová, K., Křůmal, K., Večeřa, Z. and Urban, O.: Fluxes of biogenic volatile organic compounds
639 above temperate Norway spruce forest of the Czech Republic. *Agric. For. Meteorol.* 232, 500–513,
640 <https://doi.org/10.1016/j.agrformet.2016.10.005>, 2017.
641
- 642 Kaltsonoudis, C., Kostenidou, E., Florou, K., Psichoudaki, M., and Pandis, S. N.: Temporal variability
643 and sources of VOCs in urban areas of the eastern Mediterranean, *Atmos. Chem. Phys.*, 16, 14825–
644 14842, <https://doi.org/10.5194/acp-16-14825-2016>, 2016.
645
- 646 Karl, T., Gohm, A., Rotach, M., Ward, H., Graus, M., Cede, A., Wohlfahrt, G., Hammerle, A., Haid,
647 M., Tiefengraber, M., Lamprecht, C., Vergeiner, J., Kreuter, A., Wagner, J. and Staudinger, M.:
648 Studying Urban Climate and Air quality in the Alps - The Innsbruck Atmospheric Observatory, *B. Am.*
649 *Meteorol. Soc.*, 101/4, E488 - E507, <https://doi.org/10.1175/BAMS-D-19-0270.1>, 2020.
650
- 651 Karl, T., Striednig, M., Graus, M., Hammerle, A. and Wohlfahrt, G.: Urban flux measurements reveal a
652 large pool of oxygenated volatile organic compound emissions., *PNAS*, 115/6, 1186-1191,
653 <https://doi.org/10.1073/pnas.1714715115>, 2018.
654
- 655 Kesselmeier, J. and Staudt, M.: Biogenic volatile organic compounds (VOC): an overview on emission,
656 physiology and ecology, *J. Atmos. Chem.* 33, 23–88, <https://doi.org/10.1023/A:1006127516791>, 1999.
657
- 658 Kljun, N., P. Calanca, M. W. Rotach, and H. P. Schmid, 2015: A simple two- dimensional
659 parameterisation for flux footprint prediction (FFP). *Geosci. Model Dev.*, 8, 3695–3713,
660 <https://doi.org/10.5194/gmd-8-3695-2015>.
661
- 662 Kota S. H., Park, C., Hale, M. C., Werner, N. D., Schade, G. W. and Ying, Q.: Estimation of VOC
663 emission factors from flux measurements using a receptor model and footprint analysis, *Atmos.*
664 *Environ.*, 82, 24-35, <https://doi.org/10.1016/j.atmosenv.2013.09.052>, 2014.
665
- 666 Langford, B., Misztal, P.K., Nemitz, E., Davison, B., Helfter, C., Pugh, T.A.M., MacKenzie, A.R., Lim,
667 S.F. and Hewitt, C.N.: Fluxes and concentrations of volatile organic compounds from a South-East
668 Asian tropical rainforest, *Atmos. Chem. Phys.*, 10, 8391-8412, [https://doi.org/10.5194/acp-10-8391-](https://doi.org/10.5194/acp-10-8391-2010)
669 2010, 2010.
670
- 671 Laothawornkitkul, J., Taylor, J.E., Paul, N.D., and Hewitt, C.N.: Biogenic volatile organic compounds
672 in the Earth system, *New Phytol*, 183, 27–51, <https://doi.org/10.1111/j.1469-8137.2009.02859.x>, 2009.
673



- 674 Li, D., Chen, Y., Shi, Y., He, X., Chen, X.: Impact of elevated CO₂ and O₃ concentrations on biogenic
675 volatile organic compounds emissions from Ginkgo biloba, *Bull. Environ. Contam. Toxicol.*, 82(4):473-
676 7, <https://doi.org/10.1007/s00128-008-9590-7>, 2009.
- 677
- 678 Livesley, S. J., McPherson, G. M., and Calfapietra, C.: The urban forest and ecosystem services:
679 impacts on urban water, heat, and pollution cycles at the tree, street, and city scale, *J. Environ. Qual.*,
680 45, 119–124, <https://doi.org/10.2134/jeq2015.11.0567>, 2016.
- 681
- 682 Loreto, F., Ciccioli, P., Brancaleoni, E., Valentini, R., Lillis, M.D., Csiky, O. and Seufert, G.: A
683 hypothesis on the evolution of isoprenoid emission by oaks based on the correlation between emission
684 type and Quercus taxonomy, *Oecologia*, 115, 302-305, <https://doi.org/10.1007/s004420050520>, 1998.
- 685
- 686 Monson, R.K. and Fall, R.: Isoprene emission from aspen leaves. The influence of environment and
687 relation to photosynthesis and photorespiration. *Plant Physiology*, 90, 267-274,
688 <https://doi.org/10.1104/pp.90.1.267>, 1989.
- 689
- 690 Niinemets U, Mild versus severe stress and BVOCs: thresholds, priming and consequences, *Trends*
691 *Plant Sci.*, 15(3),145-53, <https://doi.org/10.1016/j.tplants.2009.11.008>, 2010.
- 692
- 693 Noe, S. M., Penuelas, J., and Niinemets, U.: Monoterpene emissions from ornamental trees in urban
694 areas: a case study of Barcelona, Spain, *Plant Biology*, 10, 163–169, 2008.
- 695
- 696 Nowak, D., Crane, D., Stevens, J., and Ibarra, M.: Brooklyn’s Urban Forest, Report NE- 29050-53,
697 2002.
- 698
- 699 Owen, S. M., MacKenzie, A. R., Stewart, H., Donovan, R., and Hewitt, C. N.: Biogenic volatile organic
700 compound (VOC) emission estimates from an urban tree canopy, *Ecol. Appl.*, 13, 927–938,
701 <https://doi.org/10.1890/01-5177>, 2003.
- 702
- 703 Palmer, P.I., Abbot, D.S., Fu, T.-M., Jacob, D.J., Chance, K., Kurosu, T.P., Guenther, A., Wiedinmyer,
704 C., Stanton, J.C., Pilling, M.J., Pressley, S., Lamb, B., Sumner, A.L.: Quantifying the seasonal and
705 interannual variability of North American isoprene emissions using satellite observations of the
706 formaldehyde column, *J. Geophys. Res.*, 111, D12315, <https://doi.org/10.1029/2005JD006689>, 2006.
- 707
- 708 Papież, M. R., Potosnak, M. J., Goliff, W. S., Guenther, A. B., Matsunaga, S. N. and Stockwell, W. R.,
709 The impacts of reactive terpene emissions from plants on air quality in Las Vegas, Nevada, *Atmos.*
710 *Environ.*, 43, 27, 4109-4123, <https://doi.org/10.1016/j.atmosenv.2009.05.048>, 2009.
- 711
- 712 Park, C., Schade, G. W., and Boedeker, I.: Flux measurements of volatile organic compounds by the
713 relaxed eddy accumulation method combined with a GC-FID system in urban Houston, Texas, *Atmos.*
714 *Environ.*, 44, 2605–2614, <https://doi.org/10.1016/j.atmosenv.2010.04.016>, 2010.
- 715



- 716 Pegoraro, E., Rey, A., Bobich, E.G., Barron-Gafford, G.A., Grieve, K.A., Mahli, Y. and Murthy, R.:
717 Effect of elevated CO₂ concentration and vapour pressure deficit on isoprene emission from leaves of
718 *Populus deltoides* during drought, *Funct. Plant Biol.*, 31, 1137-1147, <https://doi.org/10.1071/FP04142>,
719 2004a.
- 720
- 721 Pegoraro, E., Rey, A., Greenberg, J., Harley, P., Grace, J., Mahli, Y. and Guenther, A.: Effect of
722 drought on isoprene emission rates from leaves of *Quercus virginiana* Mill, *Atmos. Environ.*, 38, 6149-
723 6156, <https://doi.org/10.1016/j.atmosenv.2004.07.028>, 2004b.
- 724
- 725 Poisson, N., Kanakidou, M., Bonsang, B., Behmann, T., Burrows, J.P., Fischer, H., Gölz, C., Harder,
726 H., Lewis, A., Moortgat, G.K., Nunes, T., Pio, C.A., Platt, U., Sauer, F., Schuster, G., Seakins, P.,
727 Senzig, J., Seuwen, R., Trapp, D., Volz-Thomas, A., Zenker, T. and Zitzelberger, R.: The impact of
728 natural non-methane hydrocarbon oxidation on the free radical and ozone budgets above a eucalyptus
729 forest, *Chemosphere - Global Change Science*, 3, 353-366, [https://doi.org/10.1016/S1465-](https://doi.org/10.1016/S1465-9972(01)00016-2)
730 [9972\(01\)00016-2](https://doi.org/10.1016/S1465-9972(01)00016-2), 2001.
- 731
- 732 Potosnak, M.J., LeSturgeon, L., Pallardy, S.G., Hosman, K.P., Gu, L., Karl, T., Geron, C. and
733 Guenther, A.B.: Observed and modeled ecosystem isoprene fluxes from an oak-dominated temperate
734 forest and the influence of drought stress, *Atmos. Environ.*, 84, 314-322,
735 <https://doi.org/10.1016/j.atmosenv.2013.11.055>, 2014.
- 736
- 737 Piccot, S., Watson, J., and Jones, J.: A global inventory of volatile organic compound emissions from
738 anthropogenic sources, *J. Geophys. Res.*, 97, 9897–9912, <https://doi.org/10.1029/92JD00682>, 1992.
- 739
- 740 Pressley, S., Lamb, B., Westberg, H., Flaherty, J., Chen, J. and Vogel, C.: Long-term isoprene flux
741 measurements above a northern hardwood forest, *J. Geophys. Res.*, 110, D7,
742 <https://doi.org/10.1029/2004JD005523>, 2005.
- 743
- 744 Rantala, P., Järvi, L., Taipale, R., Laurila, T. K., Patokoski, J., Kajos, M. K., Kurppa, M., Haapanala, S.,
745 Siivola, E., Petäjä, T., Ruuskanen, T. M., and Rinne, J.: Anthropogenic and biogenic influence on VOC
746 fluxes at an urban background site in Helsinki, Finland, *Atmos. Chem. Phys.*, 16, 7981–8007,
747 <https://doi.org/10.5194/acp-16-7981-2016>, 2016.
- 748
- 749 Reichle, R., De Lannoy, G., Koster, R. D., Crow, W. T., Kimball, J. S. and Liu, Q.: SMAP L4 Global 3-
750 hourly 9 km EASE-Grid Surface and Root Zone Soil Moisture Geophysical Data, Version 4. Boulder,
751 Colorado USA, NASA National Snow and Ice Data Center Distributed Active Archive Center,
752 <https://doi.org/10.5067/KPJNN2GI1DQR>, 2018.
- 753
- 754 Ren Y., Qu Z., Du Y., Xu R., Ma D., Yang G., Shi Y., Fan X., Tani A., Guo P., Ge Y. and Chang J.: Air
755 quality and health effects of biogenic volatile organic compounds emissions from urban green spaces
756 and the mitigation strategies, *Environ Pollut.*, 230, 849-861,
757 <https://doi.org/10.1016/j.envpol.2017.06.049>, 2017.



- 758
759 Riipinen, I., Yli-Juuti, T., Pierce, J.R., Petäjä, T., Worsnop, D.R., Kulmala, M., and Donahue, N.M.:
760 The contribution of organics to atmospheric nanoparticle growth, *Nat. Geosci.* 5, 453–458,
761 <https://doi.org/10.1038/ngeo1499>, 2012.
762
763 Rosenstiel, T. N., Ebbets, A. L., Khatri, W. C., Fall, R., and Monson, R.K.: Induction of Poplar Leaf
764 Nitrate Reductase: A Test of Extrachloroplastic Control of Isoprene Emission Rate, *Plant Biology*, 6,
765 12-21, <https://doi.org/10.1055/s-2003-44722>, 2008.
766
767 Seco, R., Karl, T., Guenther, A., Hosman, K.P., Pallardy, S.G., Gu, L., Geron, C., Harley, P. and Kim,
768 S.: Ecosystem-scale VOC fluxes during an extreme drought in a broad-leaf temperate forest of the
769 Missouri Ozarks (central USA), *Glob. Change Biol.*, 21, 3657-3674, <https://doi.org/10.1111/gcb.12980>,
770 2015.
771
772 Simon, H., Fallmann, J., Kropp, T., Tost, H. and Bruse: M. Urban Trees and Their Impact on Local
773 Ozone Concentration—A Microclimate Modeling Study, *Atmosphere*, 10, 154,
774 <https://doi.org/10.3390/atmos10030154>, 2019.
775
776 Simon, M., Dada, L., Heinritzi, M., Scholz, W., Stolzenburg, D., Fischer, L., Wagner, A. C., Kürten, A.,
777 Rörup, B., He, X.-C., Almeida, J., Baalbaki, R., Baccharini, A., Bauer, P. S., Beck, L., Bergen, A.,
778 Bianchi, F., Bräkling, S., Brilke, S., Caudillo, L., Chen, D., Chu, B., Dias, A., Draper, D. C., Duplissy,
779 J., El-Haddad, I., Finkenzeller, H., Frege, C., Gonzalez-Carracedo, L., Gordon, H., Granzin, M., Hakala,
780 J., Hofbauer, V., Hoyle, C. R., Kim, C., Kong, W., Lamkaddam, H., Lee, C. P., Lehtipalo, K.,
781 Leiminger, M., Mai, H., Manninen, H. E., Marie, G., Marten, R., Mentler, B., Molteni, U., Nichman, L.,
782 Nie, W., Ojdanic, A., Onnela, A., Partoll, E., Petäjä, T., Pfeifer, J., Philippov, M., Quéléver, L. L. J.,
783 Ranjithkumar, A., Rissanen, M. P., Schallhart, S., Schobesberger, S., Schuchmann, S., Shen, J., Sipilä,
784 M., Steiner, G., Stozhkov, Y., Tauber, C., Tham, Y. J., Tomé, A. R., Vazquez-Pufleau, M., Vogel, A.
785 L., Wagner, R., Wang, M., Wang, D. S., Wang, Y., Weber, S. K., Wu, Y., Xiao, M., Yan, C., Ye, P.,
786 Ye, Q., Zauner-Wieczorek, M., Zhou, X., Baltensperger, U., Dommen, J., Flagan, R. C., Hansel, A.,
787 Kulmala, M., Volkamer, R., Winkler, P. M., Worsnop, D. R., Donahue, N. M., Kirkby, J., and Curtius,
788 J.: Molecular understanding of new-particle formation from α -pinene between -50 and $+25$ °C, *Atmos.*
789 *Chem. Phys.*, 20, 9183–9207, <https://doi.org/10.5194/acp-20-9183-2020>, 2020.
790
791 Steinbrecher, R., Smiatek, G., Köble, R., Seufert, G., Theloke, J., Hauff, K., Ciccioli, P., Vautard, R.
792 and Curci, G.: Intra- and inter-annual variability of VOC emissions from natural and semi e natural
793 vegetation in Europe and neighbouring countries, *Atmos. Environ.*, 43, 1380e1391,
794 <https://doi.org/10.1016/j.atmosenv.2008.09.072>, 2009.
795
796 Stewart, H. E., Hewitt, C.N., Bunce R. G. H., Steinbrecher R., Smiatek G. and Schoenemeyer, T.: A
797 highly spatially and temporally resolved inventory for biogenic isoprene and monoterpene emissions:
798 Model description and application to Great Britain., *J. Geophys. Res.*, 108(D20), 4644,
799 [doi:10.1029/2002JD002694](https://doi.org/10.1029/2002JD002694), 2003.



- 800
801 Striednig, M., Graus, M., Märk, T. D., and Karl, T. G.: InnFLUX – an open-source code for
802 conventional and disjunct eddy covariance analysis of trace gas measurements: an urban test case,
803 *Atmos. Meas. Tech.*, 13, 1447–1465, <https://doi.org/10.5194/amt-13-1447-2020>, 2020.
804
- 805 Sulzer, P., Hartungen, E., Hanel, G., Feil, S., Winkler, K., Mutschlechner, P., Haidacher, S.,
806 Schottkowsky, R., Gunsch, D., Seehauser, H., Striednig, M., Juerschik, S., Breiev, K., Lanza, M.,
807 Herbig, J., Maerk, L., Maerk, T., Jordan, A.: A Proton Transfer Reaction-Quadrupole interface Time-
808 Of-Flight Mass Spectrometer (PTR-QiTOF): High speed due to extreme sensitivity, *Int. J. Mass*
809 *Spectrom.*, 368, 1–5, <https://doi.org/10.1016/j.ijms.2014.05.004>, 2014.
810
- 811 Tattini, M., Loreto, F., Fini, A., Guidi, L., Brunetti, C., Velikova, V., Gori, A. and Ferrini, F.,
812 Isoprenoids and phenylpropanoids are part of the antioxidant defense orchestrated daily by drought-
813 stressed *Platanus × acerifolia* plants during Mediterranean summers, *New Phytol.*, 207, 613-626.
814 <https://doi.org/10.1111/nph.13380>, 2015.
815
- 816 Tawfik, A.B., Stöckli, R., Goldstein, A., Pressley, S. and Steiner, A.L.: Quantifying the contribution of
817 environmental factors to isoprene flux interannual variability, *Atmos. Environ.*, 54, 216-224,
818 <https://doi.org/10.1016/j.atmosenv.2012.02.018>, 2012.
819
- 820 Thunis, P. and Cuvelier, C.: Impact of biogenic emissions on ozone formation in the Mediterranean area
821 - a BEMA modelling study, *Atmos. Environ.*, 34, 467-481, [https://doi.org/10.1016/S1352-](https://doi.org/10.1016/S1352-2310(99)00313-1)
822 [2310\(99\)00313-1](https://doi.org/10.1016/S1352-2310(99)00313-1), 2000.
823
- 824 Tsigaridis, K., and Kanakidou, M.: Importance of volatile organic compounds photochemistry over a
825 forested area in central Greece, *Atmos. Environ.*, 36, 3137-3146, [https://doi.org/10.1016/S1352-](https://doi.org/10.1016/S1352-2310(02)00234-0)
826 [2310\(02\)00234-0](https://doi.org/10.1016/S1352-2310(02)00234-0), 2002.
827
- 828 Valach, A. C., Langford, B., Nemitz, E., MacKenzie, A. R., and Hewitt, C. N.: Seasonal and diurnal
829 trends in concentrations and fluxes of volatile organic compounds in central London, *Atmos. Chem.*
830 *Phys.*, 15, 7777–7796, <https://doi.org/10.5194/acp-15-7777-2015>, 2015.
831
- 832 Vaughan, A. R., Lee, J. D., Shaw, M. D., Misztal, P. K., Metzger, S., Vieno, M., Davison, B., Karl, T.
833 G., Carpenter, L. J., Lewis, A. C., Purvis, R. M., Goldstein, A. H. and Hewitt, C. N.: VOC emission
834 rates over London and South East England obtained by airborne eddy covariance, *Faraday Discuss.*,
835 200, 599–620, <https://doi.org/10.1039/c7fd00002b>, 2017.
836
- 837 Wagner, P. and Kuttler, W.: Biogenic and anthropogenic isoprene in the near-surface urban atmosphere
838 — A case study in Essen, Germany, *Sci. Tot. Environ.*, 475, 104-115,
839 <https://doi.org/10.1016/j.scitotenv.2013.12.026>, 2014.
840



- 841 Wang, Q., Han, Z., Wang, T. and Higano, Y.: An Estimate of Biogenic Emissions of Volatile Organic
842 Compounds during Summertime in China, *Env. Sci. Poll. Res. Int.*, 14, 69–75
843 <https://doi.org/10.1065/espr2007.02.376>, 2007.
844
- 845 Wang, J.-L., Chew, C., Chang, C.-Y., Liao, W.-C., Lung, S.-C. C., Chen, W.-N., Lee, P.-J., Lin, P.-H.
846 and Chang, C.-C.: Biogenic isoprene in subtropical urban settings and implications for air quality,
847 *Atmos. Environ.*, 79, 369-379, <https://doi.org/10.1016/j.atmosenv.2013.06.055>, 2013.
848
- 849 Warneke, C., de Gouw, J. A., Del Negro, L., Brioude, J., McKeen, S., Stark, H., Kuster, W. C., Goldan,
850 P. D., Trainer, M., Fehsenfeld, F. C., Wiedinmyer, C., Guenther, A. B., Hansel, A., Wisthaler, A., Atlas,
851 E., Holloway, J. S., Ryerson, T. B., Peischl, J., Huey, L. G. and Case Hanks, A. T.: Biogenic emission
852 measurement and inventories determination of biogenic emissions in the eastern United States and
853 Texas and comparison with biogenic emission inventories, *J. Geophys. Res.*, 115, D00F18,
854 <https://doi.org/10.1029/2009JD012445>, 2010.
855
- 856 Wu, C., Pullinen, I., Andres, S., Carriero, G., Fares, S., Goldbach, H., Hacker, L., Kasal, T., Kiendler-
857 Scharr, A., Kleist, E., Paoletti, E., Wahner, A., Wildt, J. and Mentel, T.F.: Impacts of soil moisture on
858 de-novo monoterpene emissions from European beech, Holm oak, Scots pine, and Norway spruce,
859 *Biogeosciences*, 12, 177-191, <https://doi.org/10.5194/bg-12-177-2015>, 2015.
860
- 861 Yadav, R., Sahu, L.K., Tripathi, N., Pal, D., Beig, G. and Jaaffrey, S.N.A.: Investigation of emission
862 characteristics of NMVOCs over urban site of western India, *Environ. Pollution*, 252, 245-255,
863 <https://doi.org/10.1016/j.envpol.2019.05.089>., 2019.
864

865
866 **Table 1. Literature values of the 44 most abundant tree species found in the 1 km² area surrounding the measurement site. All**
867 **values are given in mg g(dry weight)⁻¹ h⁻¹. Reference subscripts refer to a) Stewart et al., 2003, b) Kesselmeier & Staudt 1999, c)**
868 **Karl et al. 2009, d) Noe et al. 2009, e) Nowak et al. 2002, f) Wang et al. 2007, g) Baghi et al 2012, h) Li et al 2009, i) Owen et al.**
869 **2003, *) standard value of 0.1, as no literature value available.**

plant species name	number of trees	ISO emission potential	MT emission potential	SQT emission potential
<i>Acer platanoides</i>	202	0.02 ^{a)}	1.83 ^{a)}	0.1 ^{c)}
<i>Betula pendula</i>	151	0.05 ^{a)}	2.80 ^{a)}	2 ^{c)}
<i>Aesculus hippocastanum</i>	98	0.10 ^{a)}	0.10 ^{a)}	0.1 ^{*)}
<i>Fagus sylvatica</i>	97	0.01 ^{a)}	0.36 ^{a)}	0.1 ^{c)}
<i>Fraxinus excelsior</i>	90	0.00 ^{a)}	0.00 ^{a)}	0.1 ^{c)}



<i>Prunus avium</i>	85	0.10 ^{a)}	0.24 ^{a)}	0.1 ^{c)}
<i>Robinia pseudoacacia</i>	85	11.87 ^{b),c),d)}	2.48 ^{b),c),d)}	0.1 ^{c)}
<i>Acer pseudoplatanus</i>	77	0.00 ^{a)}	0.00 ^{a)}	0.1 ^{c)}
<i>Picea abies</i>	68	1.07 ^{a)}	4.00 ^{a)}	0.1 ^{c)}
<i>Pinus sylvestris</i>	68	0.10 ^{a)}	6.45 ^{a)}	0.1 ^{c)}
<i>Tilia platyphyllos</i>	54	5.50 ^{a)}	0.10 ^{a)}	0.1 ^{c)}
<i>Taxus baccata</i>	52	0.10 ^{a)}	0.10 ^{a)}	0.1 ^{*)}
<i>Cornus mas</i>	40	0.10 ^{e)}	1.60 ^{e)}	0.1 ^{*)}
<i>Populus alba</i>	40	53.00 ^{a)}	2.30 ^{a)}	0.1 ^{c)}
<i>Prunus cerasifera</i>	37	0.10 ^{a)}	0.79 ^{a)}	0.1 ^{*)}
<i>Quercus robur</i>	36	38.45 ^{a)}	0.94 ^{a)}	0.1 ^{c)}
<i>Populus nigra</i>	35	52.50 ^{a)}	2.30 ^{a)}	0.1 ^{c)}
<i>Cupressus sp</i>	32	0.10 ^{a)}	0.90 ^{a)}	0.1 ^{c)}
<i>Carpinus betulus</i>	30	0.10 ^{a)}	0.04 ^{a)}	0.1 ^{c)}
<i>Acer campestre</i>	29	0.05 ^{a)}	0.10 ^{a)}	0.1 ^{c)}
<i>Salix alba</i>	24	37.20 ^{a)}	1.10 ^{a)}	0.1 ^{c)}
<i>Platanus acerifolia</i>	22	20.00 ^{a)}	0.05 ^{a)}	0.1 ^{*)}
<i>Tilia cordata</i>	21	0.00 ^{a)}	0.00 ^{a)}	0.1 ^{c)}
<i>Prunus serrulata</i>	18	0.10 ^{a)}	0.79 ^{a)}	0.1 ^{*)}
<i>Acer saccharinum</i>	17	0.10 ^{b)}	2.85 ^{b),c)}	0.1 ^{*)}
<i>Cupressus sempervirens</i>	15	0.00 ^{c)}	0.70 ^{c)}	0.1 ^{c)}
<i>Abies alba</i>	14	1.00 ^{c)}	1.50 ^{c)}	0.1 ^{c)}
<i>Pinus cembra</i>	14	0.00 ^{c)}	2.50 ^{c)}	0.1 ^{c)}
<i>Sophora japonica</i>	14	10.00 ^{f)}	0.10 ^{f)}	0.025 ^{*)}
<i>Thuja occidentalis</i>	14	0.00 ^{c)}	0.60 ^{c)}	0.025 ^{c)}
<i>Ginkgo biloba</i>	11	0.30 ^{h)}	0.60 ^{h)}	0.025 ^{*)}
<i>Malus domestica</i>	11	0.50 ^{a)}	0.60 ^{a)}	0.025 ^{c)}
<i>Sorbus aucuparia</i>	11	0.50 ^{a)}	0.10 ^{a)}	0.025 ^{c)}
<i>Gleditsia triacanthos</i>	10	0.10 ^{e)}	0.70 ^{g),e)}	0.025 ^{*)}
<i>Sorbus intermedia</i>	10	0.50 ^{a)}	3.00 ^{a)}	0.025 ^{*)}
<i>Aesculus</i>	8	0.00 ^{g)}	12.00 ^{g)}	0.025 ^{*)}



<i>carnea</i>				
<i>Chamaecyparis lawsoniana</i>	8	0.10 ⁱ⁾	0.67 ⁱ⁾	0.025 [*])
<i>Liquidambar styraciflua</i>	8	46.58 ^{b)}	19.17 ^{b)}	0.025 [*])
<i>Magnolia Kobus</i>	8	0.05 ^{a)}	3.25 ^{a)}	0.025 [*])
<i>Platanus hispanica</i>	8	20.00 ^{a)}	0.05 ^{a)}	0.025 [*])
<i>Acer palmatum</i>	7	0.05 ^{a)}	1.83 ^{a)}	0.025 [*])
<i>Juglans regia</i>	7	0.00 ^{b)}	1.40 ^{b), c)}	0.025 ^{c)}
<i>Larix decidua</i>	7	0.00 ^{c)}	5.00 ^{c)}	0.025 ^{c)}
<i>Platanus occidentalis</i>	7	20.00 ^{a)}	0.05 ^{a)}	0.025 ^{c)}

870